

Preparation, structure, and composition of ordered tin-oxide overlayers on the Au(111) surface

Y. Zhang and A. J. Slavin

*Department of Physics, Trent University, Peterborough, Ontario, Canada K9J 7B8
and Department of Physics, Queen's University, Kingston, Ontario, Canada K7L 3N6*

(Received 12 October 1992; revised manuscript received 24 June 1993)

Previous work has described the growth mode of tin deposits on the Au(111) surface and the subsequent oxidation of the tin at room temperature. Because the gold does not oxidize under the conditions of this experiment, one can monitor the growth of the oxide layer in an incremental fashion. This paper extends the study to oxidation at higher temperatures. From 500 to 800 K at about 10^{-6} Torr of oxygen, at least half the tin in-diffuses, with the rest forming an ordered SnO₂ layer on the surface. This ordered oxide has no counterpart for bulk tin, which melts at 505 K. Heating above 800 K causes diffusion of the remaining tin and oxygen into the gold substrate. The formation of the oxide layer has been studied by Auger spectroscopy, electron-energy-loss spectroscopy, work-function measurements, and low-energy-electron diffraction.

I. INTRODUCTION

The study of the oxidation of thin metal films is interesting in a number of respects. For example, the comparison of the oxidation of thin metal films and that of corresponding bulk materials can provide a better understanding about the growth of a metal oxide on a bulk sample.¹⁻³ Second, many bulk metal oxides lack stable crystal faces and are hard to grow. It has been reported that annealing oxidized metal films can sometimes produce well-ordered oxide films, which are alternatives to the bulk oxide material for surface studies, and possibly for chemical catalysis.⁴

Oxidation of metal films on metal substrates has been investigated for various adsorbate-substrate combinations.⁴ Among them, ordered oxide films were obtained for only a few systems.⁵⁻⁹ It has been found in this laboratory that oxidation of Sn on the Au(111) surface at room temperature leads to disordered Sn-oxide films¹⁰ which cannot be ordered by annealing. However, the present work has shown that oxidation at substrate temperatures from 500 to 700 K does provide well-ordered Sn-oxide films on the Au(111) surface. The preparation, composition, and structure of these films are discussed, aided by a comparison with measurements on an SnO₂ single crystal. Because Au does not oxidize under the conditions of this experiment (Ref. 11 and references therein), the tin oxide layers can be built up in a well-defined manner by controlling the amount of Sn deposition.

II. EXPERIMENT

The experiment was carried out under ultrahigh vacuum (UHV) conditions with a base pressure less than 5×10^{-10} Torr. The gold single crystal (99.999% pure) was cut to within 1° of the (111) plane and was spot welded to nickel wires and heated resistively. The sample was cleaned in vacuum by argon-ion bombardment while heated at 850 K, followed by a short vacuum annealing at

the same temperature. After cleaning, Sn deposition or oxidation, no contamination of the sample surface was detected by Auger electron spectroscopy (AES) within the sensitivity of the four-grid low-energy electron-diffraction (LEED)-type analyzer. Sn was deposited onto the Au(111) surface by heating a simple evaporator at 750°C. Cold-trapped ultrahigh-purity oxygen gas was introduced into the chamber through a leak valve and the purity monitored with a quadrupole mass spectrometer.

The SnO₂ single-crystal face was shown by x rays to be within 1° of the (110) plane (one of the natural growth faces) and the crystal was mechanically mounted to the sample manipulator with nickel wires. A thermocouple was spotwelded to the nickel wires so that the temperature of the sample could be monitored when the sample reached thermal steady state. The sample was cleaned by ion bombardment at 1000 K. The major contaminants were found to be carbon and potassium, which were reduced below the noise level of our detector after cleaning. Since it is believed that ion bombardment and annealing reduce SnO₂ to SnO,^{12,13} the cleaned surface was further annealed at 1000 K in the presence of oxygen (5×10^{-6} Torr) for several hours. This procedure is reported to produce a nearly perfect (110) surface.¹³ It did result in a clear low-energy electron-diffraction (LEED) pattern, as desired.

Auger spectra of the Au ($N_{6,7}VV$, 69 eV), Sn ($M_4N_{4,5}N_{4,5}$, 430 eV), and oxygen ($KL_{2,3}L_{2,3}$, 503 eV) peaks were obtained using modulation voltages of 2, 7, and 11 V (peak-to-peak), respectively, and a primary electron beam at normal incidence with an energy of 1.5 keV and a beam current of 15 μ A. Electron-energy-loss spectroscopy (EELS) data were recorded using a 3-V peak-to-peak modulation and a 0.6- μ A electron beam, with primary energy of 70 eV for Sn on Au(111) and 100 eV for the SnO₂ single-crystal sample. The EELS results are due almost totally to the surface layer, because at these primary energies the electrons have an inelastic mean free path (IMFP) close to its minimum value (typically 1.5 monolayers) and because the electrons have to pass

through the surface layer on both entry and exit. All of the measurements were recorded with a lock-in amplifier in the second harmonic mode $[dN(E)/dE]$.

Differential work-function measurements, accurate to within 0.04 eV, were made by observing the onset of the secondary electron peak.¹⁴

III. RESULTS

A. Auger electron spectroscopy

Previous studies have been carried out on the growth of Sn thin films on the Au(111) surface^{15,16} and the oxidation of these films at room temperature.¹⁰ Those results pertaining to the present paper will now be summarized. It was found that Sn forms an alloy AuSn at room temperature. When oxidized at the same temperature, Sn atoms diffused to the surface and formed disordered Sn-oxide layers. The quantity of Sn deposited was measured using plots of the Au and Sn Auger peaks as a function of the deposition time, at constant evaporation rate. The completion of the first Sn layer, after a deposition time τ , was evidenced by a clear break in slope. The quantity of Sn deposited in a time $n\tau$ will be referred to as an “ $n\tau$ ” deposit. The alloy formed by the deposition of 1τ of Sn is two atomic layers thick.¹⁵ However, it appears that the sticking probability of the Sn falls by one half after completion of the first layer, so that a 6τ deposit, for example, results in a total thickness of the alloy layer of seven atomic layers. Note that to avoid confusion between “monolayers” and atomic layers, the notation “ τ ” has been used to replace “ML” (monolayer) used in previous publications.

In the present work, Sn deposits were also made with the sample held at room temperature; oxidation was carried out at various temperatures ranging from room temperature to 800 K. For oxygen pressures from 5×10^{-8} to 1 Torr, Sn deposits were oxidized readily throughout this temperature range.

Since the Auger signal of Sn is a mixture of a metallic Sn signal and a Sn-oxide signal, the two components were separated by a simple decomposition procedure,¹ using the Sn line shapes from unoxidized Sn on Au(111) and from single-crystal SnO₂ as two basis functions. The latter line shape was essentially identical to that for fully oxidized Sn on Au(111). The results will be referred to as the “Sn” signal for the metallic component and the “SnO₂” signal for the oxide component. These decompositions gave good fits to the original data, unlike the case for oxidation at room temperature¹⁰ where two different oxides were present, and indicates that a single oxide was present for the high-temperature oxidation.

Figure 1 plots the Auger intensities (peak-to-peak height) of Au, O, Sn, and SnO₂ against the logarithm of the oxygen exposures for the oxidation of a 6τ deposit of Sn on Au(111) at 600 K and 5×10^{-6} Torr. All intensities have been divided by the value for the clean Au surface, measured before each run, to account for slight differences in primary current, etc., from run to run. No adjustment¹⁷ has been made for the different modulation voltages. In the inset in Fig. 1 the same data are plotted

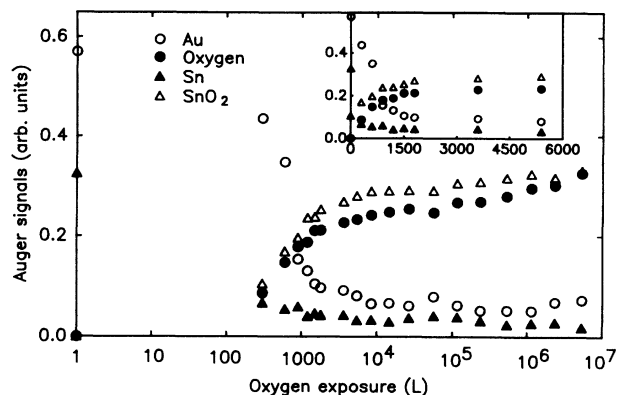


FIG. 1. Peak-to-peak Auger intensities as a function of the oxygen exposure (log scale). The inset is plotted linearly.

on a linear scale for oxygen exposures up to 6000 L (1 langmuir = 10^{-6} Torr s). The inset shows that Sn oxidizes quite rapidly initially but very slowly above 1500 L. The data for much larger exposures, to 5×10^6 L, suggest a saturation for all the curves, within the experimental scatter, except for the oxygen amplitude which continues to increase slowly. It should be noted that this saturation only implies no further change in the signal within the sampling depth of the Sn and oxygen Auger electrons, of about 4 atomic layers. It is possible that the Sn below this is not fully oxidized, for thick deposits.

For oxidation at room temperature, the total Sn Auger intensity increased from the beginning as the subsurface Sn segregated to the surface.¹⁰ However, for oxidation at 600 K the total Sn signal (Sn plus SnO₂) fell from its initial value of 0.32 in Fig. 1 to 0.17, for only a 300-L exposure. Approximately the same decrease in the Sn signal was observed when the unoxidized sample was heated to 600 K in vacuum for the same length of time. The logical explanation for the decrease in both cases is diffusion of some of the Sn atoms into the Au substrate on heating. However, during oxidation some of these Sn atoms gradually diffuse back to the surface where they are trapped by interaction with oxygen, causing the total tin signal to increase again. As will be discussed later, less than half of the tin eventually is bonded in the surface oxide, with the rest being lost by diffusion into the substrate.

Shifts in the position of the tin Auger peak and experimental values for the Au Auger signal after oxidation are recorded in Table I for a range of Sn deposits. Annealing

TABLE I. AES results for high-temperature oxidation.

Sn deposit	Sn shift (± 0.5 eV)	Au signal ^a	
		Expt.	Calc. ^b
0.5τ	3.8 eV		
1τ	5.1 eV	0.51	0.51
2τ	5.0 eV	0.41	0.36
4τ	5.0 eV	0.12	0.19
6τ	5.0 eV	0.06	0.09

^aNormalized to unity for clean Au.

^bFrom Eq. (2).

the sample above 800 K always resulted in the total loss of both tin and oxygen by in-diffusion into the substrate (no thermal desorption of either was seen during this annealing).

B. Electron-energy-loss spectroscopy

EELS spectra were taken for various Sn coverages as well as for the SnO₂ single-crystal sample. These spectra will be discussed in some detail because such spectra have been shown to be very useful in differentiating between SnO and SnO₂ (e.g., Refs. 12, 15, and 18). The EELS spectrum of the SnO₂ crystal is shown in Fig. 2, where curves are plotted both for the original dN/dE data, and as $-d^2N/dE^2$ following spline smoothing. The positions of loss energies occur in the former plot at locations of maximum negative slope; in the latter they are at the peak positions. The two sets of positions agreed in all cases, so only dN/dE spectra will be shown from here on. Figure 2 shows a Sn $N_{4,5}$ ionization loss at about 28 eV and bulk (B) and surface (S) plasmon losses at about 19 and 13.5 eV, respectively.^{18,12} These latter two losses have also been ascribed to band transitions,¹⁹ but they will be referred to here as plasmon losses. The peaks at 8.5 (X) and 6.3 (Y) eV will be discussed below.

Almost all the features in our spectrum from single-crystal SnO₂ are in good agreement with those reported by Bevolo, Verhoeven, and Noack for high-purity SnO₂ powder,¹² if we add about 1.5 eV to their peak positions to bring them into agreement with other published work.¹⁸ The only exception is a very weak peak which we see reliably at 24 eV, and which may, in fact, be present but unlabeled in Fig. 3 by Bevolo, Verhoeven, and Noack. Our peak positions are also in good agreement with those reported by de Frésart, Darville, and Gilles²⁰ for a 90-eV beam from the (110) face of an SnO₂ single crystal before ion cleaning, except that they do not report a peak at 8.4 eV. Cox and Hoflund¹⁹ have suggested that the loss peaks below 10 eV from an oxidized Sn sample were a collection of dipole-allowed transitions from the valence band to the conduction band in SnO₂. This seems to be a reasonable explanation for our peaks at 8.4 and 6.4 eV, since Robertson²¹ has shown that the SnO₂ band structure has peaks in the density of states 0.5 and 2 eV below the valence-band maximum, due mainly to oxy-

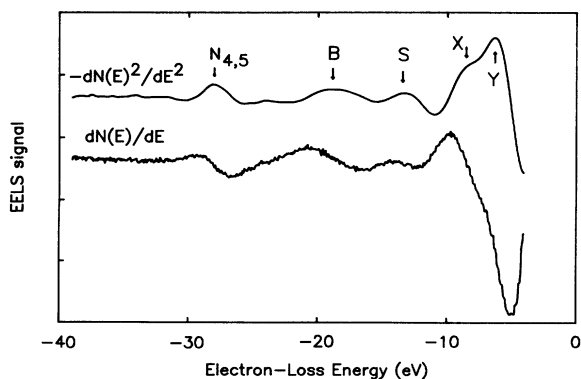


FIG. 2. Electron-energy-loss spectra for single-crystal SnO₂.

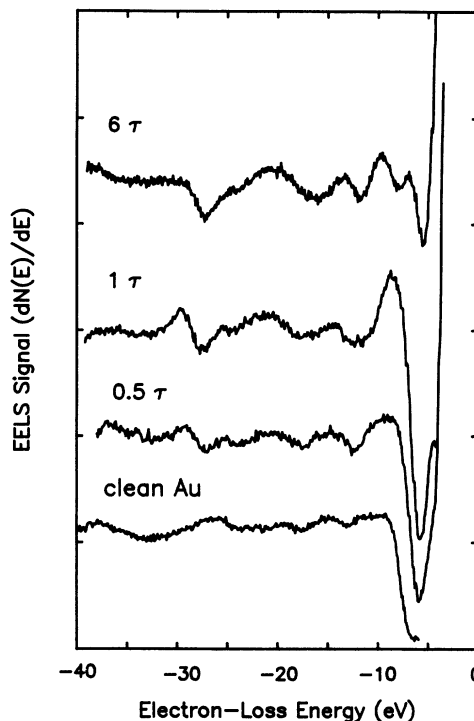


FIG. 3. Electron-energy-loss spectra for several Sn deposits, after saturation oxidation.

gen $2p$ lone-pair states, and in the conduction band (which is primarily s -like) between 6 and 7 eV above the valence-band maximum. This calculated band structure is in good agreement with the ultraviolet photoelectron study by Gobby and co-workers.^{22,21}

Figure 3 shows the EELS spectra for clean Au, and 0.5, 1, and 6- τ deposits of Sn on Au(111), after saturation oxidation at 500 to 700 K. The peak assignments for clean Au have been discussed elsewhere.^{10,23} For the oxygen-saturated deposit of 6- τ of Sn on Au(111), the EELS spectrum shows peaks at all the same positions as for the SnO₂ single-crystal sample, except for a shift of the peak at 8.4 eV to about 9.3 eV. The EELS spectra for 2 and 4 τ were essentially the same as for 6 τ . However, for 1 τ of Sn on Au a single low-energy peak near 7 eV was observed. The 0.5- τ spectrum appears to be a mixture of that for clean Au and that for an oxidized 1- τ Sn deposit. Given the high surface sensitivity of the EELS measurements in this experiment, this implies that the Au surface was only partially covered by the Sn oxide for the 0.5- τ deposit, as expected if some Sn in-diffuses on heating. The weak peak at 24 eV is probably a mixture of the loss for the bulk plasmon in gold and the weak 24 eV loss observed for SnO₂. This peak was absent in the AuSn alloy, prior to oxidation.

C. Low-energy-electron diffraction

For the clean Au(111) surface, our LEED observation showed a $p(1 \times 1)$ pattern with no reconstruction spots visible.¹⁵ The LEED pattern for deposits of Sn on the Au(111) surface has been discussed elsewhere.^{15,16} It was

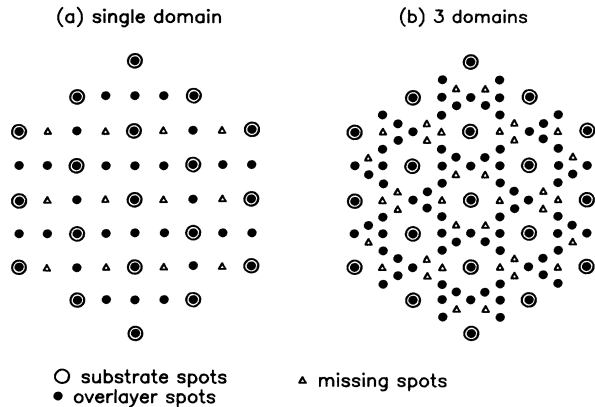


FIG. 4. Schematic of the $c(2 \times 4)$ LEED pattern.

found¹⁵ that oxidation at room temperature near 10^{-6} Torr led to disordered Sn oxide layers on the Au(111) surface with no LEED pattern except for weak Au(111) substrate spots. However, above 500-K oxidation leads to a sharp pattern observed for all Sn coverages (0.5 to 6 τ). It has a $c(2 \times 4)$ periodicity relative to the Au surface but with many spots missing, and so will be referred to as the “ $c(2 \times 4)$ ” pattern. This pattern is shown schematically in Fig. 4, where the triangles represent the spots which are missing from the $c(2 \times 4)$ pattern. The sample work function changed less than 0.2 eV on formation of the “ $c(2 \times 4)$ ” layer.

Oxidation carried out at high oxygen pressure (≈ 0.5 Torr) never resulted in an ordered oxide layer, regardless of the sample temperature.

D. Exposure of the oxide surface to large doses of oxygen

When the ordered oxide surface was exposed to a much larger oxygen dosage (0.5 Torr for 1 h) from room temperature to 700 K, a further oxygen uptake corresponding to an increase in the Auger intensity of about 50% was observed, but with no further shift in the Sn Auger peak position. This was accompanied by an increase in the work function of 1.5 eV for deposits of 2 τ or larger, and a marked increase in the background LEED intensity, although the “ $c(2 \times 4)$ ” pattern remained visible. Subsequent annealing of the sample at an oxygen pressure of 10^{-6} Torr between 500 and 700 K reduced the oxygen AES intensity to its original value and restored a clear “ $c(2 \times 4)$ ” pattern, although the spots were not quite as sharp as originally.

IV. DISCUSSION

A. Chemical composition of the oxide

Since AES does not furnish enough information to distinguish SnO from SnO₂,^{12,18} the evidence for chemical composition in this work came mainly from the EELS study. For oxidized Sn on Au(111), we suggest the composition is SnO₂ based on the similarity between the peak positions in the EELS spectrum for the SnO₂ single crys-

tal and oxidized Sn on Au(111), as seen by comparing Fig. 2 with the 6- τ spectrum of Fig. 3.

There is disagreement in the literature as to whether the surface layer on oxidized bulk tin is SnO or SnO₂, with Powell¹⁸ claiming the former and Bevolo, Verhoeven and Noack¹² the latter. The interpretation of the data is complicated by the fact that both oxides have peaks in their EELS spectra near 6, 8, and 14 eV.¹² However, the 19-eV bulk-plasmon peak from SnO₂ is unique to this oxide.¹² The presence of this peak in this work, combined with the high surface sensitivity of the 70-eV primary electrons used, clearly shows that SnO₂ is present on the surface. At the same time, the existence of a single, sharp LEED pattern and the success in fitting the Auger line shapes using a single line shape for the oxide component would seem to imply that there is only one oxide present which must, therefore, be SnO₂. This point will be discussed in more detail later. This SnO₂ layer persists to a depth of about three monolayers, as shown below. In the spectra of oxidized Sn on Au, the features below 10 eV change dramatically between the 1- τ deposit and larger deposits. This can probably be explained by changes in band structure as the oxide thickens beyond 1 monolayer.

Finally, the claim that only SnO₂ exists on this surface does not contradict the earlier studies which showed that both SnO and SnO₂ were present on bulk Sn (e.g., Refs. 10, 12, and 18). Bulk Sn melts at 505 K, so that the earlier work could not be carried out at the higher temperatures used in the present study.

B. Auger amplitudes and chemical shifts

The major feature in the Auger spectra of Sn is a doublet with the higher energy lobe at about 430 eV and a peak separation of 8.5 eV. Powell found that both SnO and SnO₂ had the same chemical shifts (5.5 eV) and almost identical structure in their Auger spectra.¹⁸ Only the peak-to-peak height ratios of the major Sn and oxygen peaks differed slightly, but for oxidized Sn these ratios are too sensitive to the exact oxygen exposure to be useful for differentiating between SnO and SnO₂. Table I shows that after saturation the chemical shift of the tin peak was close to that observed by Powell for SnO₂ except for the 0.5- τ deposit. This indicates that essentially no tin remained unoxidized within the AES sampling depth and supports the conclusions from EELS.

Table I also gives the ratios of the Au signal strengths after oxidation to the strength for clean Au. These values can be used to estimate the thickness of the oxide layer, as follows. The attenuation length λ for the 69-eV electrons from the gold substrate can be approximated from the inelastic mean free path (IMFP) through SnO₂, calculated using a prescription by Tanuma, Powell, and Penn²⁴ to have a value of 1.5 monolayers. However, the IMFP is expected to exceed λ by about 30%,²⁵ so $\lambda \approx 1.2$ monolayers. The thickness d of the oxide overlayer can now be calculated using the equation

$$S_d = S_0 \exp(-d/0.75\lambda) \quad (1)$$

where S_d is the Auger signal of Au below the oxide and

S_0 is the signal from clean Au. This calculation ignores the differences in backscattering between the two substrates, which can cause an error up to 4%.²⁶ The factor of 0.75 in the exponential accounts for the large collection angle in the LEED-type analyzer.^{27,28} This calculation gives an oxide thickness of roughly 0.6 monolayers for the $1\text{-}\tau$ tin deposit. Since this deposit is expected to have formed a layer of AuSn two atomic layers thick originally, it appears that at least half of the Sn atoms have been lost by diffusion into the Au substrate during the oxidation process. This assumes that the atomic density of Sn is approximately the same in the AuSn alloy and in the oxide. The assumption is reasonable, given that the concentration of Sn atoms in AuSn with the same atomic density of pure Au (Ref. 15) is $2.9 \times 10^{28} \text{ m}^{-3}$, while in bulk SnO_2 it is $2.8 \times 10^{28} \text{ m}^{-3}$.²⁹

An $n\text{-}\tau$ Sn deposit (for $n > 1$) results in $(n + 1)$ atomic layers of the AuSn alloy¹⁵ (see Sec. III A), and one layer of AuSn should produce one layer of SnO_2 since the density of Sn atoms is virtually the same in both. Therefore, assuming that one half of the Sn is lost by in-diffusion for all deposits, an $n\text{-}\tau$ deposit of Sn should produce $(n + 1)/2$ monolayers of oxide for $n > 1$. This rough model can be tested from the data of Table I. The transmission factor is 0.51 for Au Auger electrons through the oxide produced by a $1\text{-}\tau$ deposit; i.e., for one monolayer of oxide. Therefore, the Au intensity for an $n\text{-}\tau$ deposit ($n > 1$) should be

$$(0.51)^{(n+1)/2}. \quad (2)$$

These calculated values are listed in Table I, and are in reasonable agreement with the measured values. While not expected to be highly accurate, these results do lend support for the general model of oxide formation and in-diffusion described above.

The above model also explains how the saturation SnO_2 signal for the $6\text{-}\tau$ deposit in Fig. 1 can be slightly greater than the Sn signal before oxidation, even though some in-diffusion has occurred. Qualitatively, this is possible because the Auger signal is insensitive to tin atoms lying deeper than about three atomic layers, and because the IMFP for the Sn Auger electrons in SnO_2 is slightly larger than in AuSn. Quantitatively, λ for the Sn (430 eV) electrons in the AuSn alloy has been measured to be 3.6 monolayers.¹⁵ This value can be used to provide an estimate for the λ 's in SnO_2 by scaling by the ratio of the calculated IMFP's (Ref. 24) for SnO_2 and AuSn. This procedure gives values of 4.9 and 5.4 monolayers for the λ 's for Sn (430 eV) and O (503 eV) electrons in SnO_2 . (The bulk AuSn alloy and SnO_2 have approximately the same volume per formula unit, so no further scaling is necessary.³⁰) The Sn AES signal from seven atomic layers of the initial AuSn alloy was 0.38, normalized to the clean Au signal.¹⁵ The Sn signal from one monolayer of SnO_2 , again divided by the amplitude for clean Au, was 0.19, and the transmission factor per layer for 430-eV electrons is, from Eq. (1), $\exp[-1/(0.75 \times 4.9)] = 0.71$. Therefore the SnO_2 signal expected from about 3.5 monolayers of SnO_2 is $0.19(1 + 0.71 + 0.71^2 + 0.5 \times 0.71^3) = 0.45$. This gives a ratio with the Sn from AuSn of 1.2,

in good agreement with the measured ratio of 1.1 from Fig. 1. Note, in addition, that because the top layers contribute most to the AES signal, in-diffusion should affect tin signals for small Sn deposits much more than for large deposits. This effect is seen in a 24% decrease in the tin signal for the $1\text{-}\tau$ deposit after oxidation, compared to the 10% increase for the $6\text{-}\tau$ deposit.

Finally, it is instructive to plot the strength of the SnO_2 signal from Fig. 1 against the oxygen signal. Figure 5 shows these data as open circles. The data at lower exposures can be fitted well by the straight line shown in Fig. 5. Three points are of interest in this plot. (a) There is no visible change in slope of the experimental data until the oxide has reached a thickness of about two monolayers, calculated using the value for λ discussed above. This implies no change in oxide stoichiometry over at least this thickness. A similar plot was very nonlinear for room-temperature oxidation for which both SnO and SnO_2 occur.¹⁰ This is strong support for the claim made earlier that a single oxide is present in this study. (b) The experimental data points droop well below the straight line above a thickness of about two monolayers. This droop is too large to be explained by the small difference in the λ 's of the Sn and oxygen electrons, which should cause only a slight curvature in the curve. Rather, the droop is suspected to be due to an accumulation of oxygen on the surface, in excess of the stoichiometric value, once the oxide layer has become thick enough to impede the ingress of oxygen. This is consistent with the 50% increase in the AES intensity for oxygen when the "c(2×4)" surface was given a very large oxygen dose at 0.5 Torr. (c) The difference in the λ 's of the Sn and oxygen Auger electrons is not great enough to permit one to tell from this plot whether the oxide grows layer by layer, or nucleates and propagates laterally as a multilayer as was the case for the lead and bismuth oxides on Au.^{1,2} However, the fact that the EELS spectrum for the $1\text{-}\tau$ Sn deposit bears little resemblance to that for clean gold suggests that most, if not all, of the surface is covered by oxide at this point. If the oxide nucleated as a multilayer one would expect that a substantial part of the surface would be bare Au, especially given the loss of some Sn by in-diffusion. As well, the absence in the $1\text{-}\tau$ EELS spec-

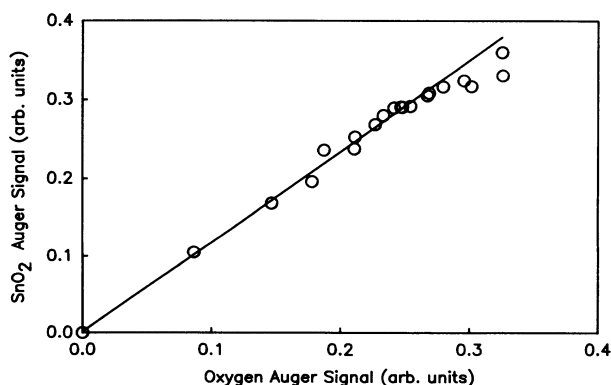


FIG. 5. Auger intensities from an oxidized $6\text{-}\tau$ Sn deposit: SnO_2 intensity vs oxygen intensity.

trum of the 8.4-eV peak seen for bulk SnO₂ indicates a very thin oxide layer.

C. Structure of the oxide overlayer

The LEED pattern has a $c(2 \times 4)$ periodicity relative to the Au(111) substrate, but with many spots missing. The absence of spots was observed at all energies and incident angles of the primary electron beam, indicating that it is caused by the atomic arrangement inside the unit cell and not by glide lines.³¹ A new method of analyzing such patterns was developed to handle this case. Using this method, we suggest that the " $c(2 \times 4)$ " unit cell contains 4 Sn and 8 oxygen atoms, with the Sn atoms lying at bridge sites and the oxygen atoms lying near top sites. A full discussion of this method and the LEED pattern will be published elsewhere.

D. High oxygen doses on the " $c(2 \times 4)$ " layer

The LEED and AES results for the large oxygen dosage (0.5 Torr for 1 h) between room temperature and 700 K, following formation of the " $c(2 \times 4)$ " oxide surface, indicate that the " $c(2 \times 4)$ " surface could still adsorb oxygen under high oxygen pressure but was not, itself, disordered in the process. The fact that annealing the heavily exposed sample in an oxygen pressure of 10^{-6} Torr at about 600 K could remove the high LEED background and reduce the oxygen AES signal to its original value suggests that the extra oxygen is only loosely bound in the near-surface region. Adsorption of this extra oxygen increased the work function by 1.5 eV. Because oxygen is strongly electronegative, this indicates that at least some of this additional oxygen lay on top of the oxide surface. [The small change (≤ 0.2 eV) in work function during formation of the " $c(2 \times 4)$ " layer is difficult to interpret in terms of the location of the oxygen, given that

the oxygen is being added at the same time that Au atoms are retreating below the surface.]

V. CONCLUSIONS

Oxidation of ultrathin Sn films on Au(111) at room temperature or at high pressure (≥ 0.5 Torr) produces disordered oxide films, which do not order with subsequent annealing. However, oxidation at high temperature (500–800 K) and low oxygen pressure (1 to 5×10^{-6} Torr) does result in fully oxidized and well-ordered Sn oxide films, but with at least 50% of Sn being lost by indiffusion during oxidation at 600 K. The composition of this oxide is SnO₂, at least in the first several layers. This technique of oxide formation is of interest *per se*, because ordered oxide layers do not form on metallic tin up to its melting temperature of 505 K. The SnO₂ layers on Au(111) have a $c(2 \times 4)$ structure, but with a number of missing spots. Subsequent higher oxygen dosage between room temperature and 700 K causes a large increase in the surface oxygen on top of the " $c(2 \times 4)$ " oxide layer; this extra oxygen can be removed by heating at 10^{-6} Torr of oxygen without significantly affecting the ordered oxide. Annealing at temperatures above 800 K causes diffusion of the Sn and oxygen into the bulk Au(111) substrate in all cases.

ACKNOWLEDGMENTS

Thanks are due to Ken Fowler for technical support and to E. Puckrin and P. Ma for many useful discussions. The generous donations of the gold crystal by Dr. M. Swanson (University of North Carolina) and the SnO₂ crystal by Professor R. Heilbig (Institut für Angewandte Physik) are much appreciated. Thanks for financial support are expressed to the Natural Sciences and Engineering Research Council of Canada, and to Queen's University for Y.Z.

¹F. Peeters and A. J. Slavin, *Surf. Sci.* **214**, 85 (1989).

²E. Puckrin and A. J. Slavin, *Phys. Rev. B* **42**, 1168 (1990).

³A. J. Slavin and E. Puckrin, *Langmuir* **7**, 2564 (1991).

⁴G. H. Vurens, M. Salmeron, and G. A. Somorjai, *Prog. Surf. Sci.* **32**, 211 (1989).

⁵K. B. Lewis, S. T. Oyama, and G. A. Somorjai, *Surf. Sci.* **233**, 75 (1990).

⁶G. H. Vurens, M. Salmeron, and G. A. Somorjai, *Surf. Sci.* **201**, 129 (1988).

⁷R. M. Nix, Robert W. Judd, and Richard M. Lambert, *Surf. Sci.* **205**, 59 (1988).

⁸U. Bardi, P. N. Ross, and G. A. Somorjai, *J. Vac. Sci. Technol. A* **2**, 40 (1984).

⁹J. P. S. Badyal, A. J. Gellman, R. W. Judd, and R. M. Lambert, *Catal. Lett.* **1**, 41 (1988).

¹⁰Y. Zhang and A. J. Slavin, *J. Vac. Sci. Technol. A* **10**, 2371 (1992).

¹¹J. G. MacMillan-Jones, F. A. Londry and A. J. Slavin, *Surf. Sci.* **186**, 357 (1987).

¹²A. J. Bevolo, J. D. Verhoeven, and M. Noack, *Surf. Sci.* **134**, 499 (1983).

¹³D. F. Cox, T. B. Fryberger, and S. Semancik, *Surf. Sci.* **224**, 121 (1989).

¹⁴G. Bachmann, J. Scholtes, and H. Oechsner, *Mikrochim. Acta (Wein)* **1**, 1853 (1972).

¹⁵Y. Zhang and A. J. Slavin, *J. Vac. Sci. Technol. A* **9**, 1784 (1991).

¹⁶M.-G. Barthès and C. Pariset, *Thin Solid Films* **77**, 305 (1981).

¹⁷N. J. Taylor, *Rev. Sci. Instrum.* **40**, 792 (1969).

¹⁸R. A. Powell, *Appl. Surf. Sci.* **2**, 397 (1979).

¹⁹D. F. Cox and G. B. Hoflund, *Surf. Sci.* **151**, 202 (1985).

²⁰E. de Frésart, J. Darville, and J. M. Gilles, *Solid State Commun.* **37**, 13 (1980).

²¹J. Robertson, *J. Phys. C* **12**, 4767 (1979).

²²P. L. Gobby and G. J. Lepeyre, in *13th Conference on Physics of Semiconductors*, edited by F. G. Fumi (North-Holland, Amsterdam, 1976).

²³S. Singh, Ph.D. thesis, University of Keele, 1976.

²⁴S. Tanuma, C. J. Powell, and D. R. Penn, *J. Vac. Sci. Technol. A* **8**, 2213 (1990).

²⁵A. Jablonski, *Surf. Sci.* **188**, 164 (1987).

²⁶D. Ze-jun, R. Shimizu, and S. Ichimura, *Surf. Interf. Anal.* **10**,

- 253 (1987).
- ²⁷M. P. Seah, *Surf. Sci.* **32**, 703 (1972).
- ²⁸E. Puckrin and A. J. Slavin, *J. Electron Spectrosc. Relat. Phenom.* **57**, 202 (1991).
- ²⁹R. Wyckoff, *Crystal Structures* (Wiley, New York, 1963), Vol. 1.
- ³⁰M. P. Seah and W. A. Dench, *Surf. Interface Anal.* **1**, 2 (1979).
- ³¹W. S. Yang and F. Jona, *Phys. Rev. B* **29**, 899 (1984).